Monograph:
Zhao, Ling, Zheng, Ying and Mayhew, J.E.W. (1997) An Evaluation of the Nonlinear MultiComponent Analysis Technique for Reflection Spectra. Research Report. ACSE Research Report 685 . Department of Automatic Control and Systems Engineering

An Evaluation of the Nonlinear MultiComponent Analysis Technique for Reflection Spectra

Ling Zhao#, Ying Zheng#, and J.E.W. Mayhew*

#Department of Automatic Control and Systems Engineering
Sheffield University
*AI Vision Research Unit, Department of Psychology
Sheffield University

Research Report Number: 685

August 1997

An Evaluation of the Nonlinear MultiComponent Analysis Technique for Reflection Spectra

Ling Zhao #, Ying Zheng #, and J. E. W. Mayhew *

Department of Automatic Control and Systems Engineering, Sheffield University

* AI Vision Research Uint, Department of Psychology, Sheffield University

Abstract: Analysis of the absorption spectra in the visible range has made it possible to monitor the oxygen supply and metabolism of organic tissues continuously and non-invasively. The nonlinear multicomponent analysis (NLMCA) is an evaluation method for the reflection spectra of the tissues. In this report, the derivation of the relation between the reflection and absorption spectra based upon Kubelka-Munk theory is reviewed to introduce the foundation of the NLMCA technique. Then, the procedures of the NLMCA algorithm are described and simulation studies are performed. The results indicate that the NLMCA algorithm generally works well after a minor modification but is sensitive to modelling errors due to invalid assumptions on the scattering properties of samples. A direct algorithm based on linear least squares is then suggested to deal with the same problem and simulation studies are performed to make a comparision with the NLMCA algorithm, which demonstrate better robust properties of the alternative strategy.

1. Introduction

The redox state of the respiratory chain gives information about the oxygen supply and metabolism of living organisms. Due to some members of the respiratory chain such as hemoglobin, myoglobin, and cytochromes having characteristic absorption spectra in the visible range, spectrophotometric methods have been used to study the redox states in vivo. This makes it possible to monitor the oxygen supply and metabolism of organic tissues continuously and non-invasively.

For now, the technical developments have allowed a sufficiently accurate measurement of reflection spectra of organisms which are under an illumination of

light. However, the question of correct evaluation of the spectra has only partly been solved. One class of typical evaluation methods for the reflection spectra of biological materials are the two-flux evaluation methods of multicomponent systems originally developed based upon the Kubelka-Munk (1931) theory (Hoffman et al. 1984 and 1985). Apart from these, there are also the methods of dual wavelength evaluation and reference spectra which were reported by Chance and Williams (1955) and Figulla et al. (1983), respectively. In Hoffmann and Lubbers (1986), the validity and limits of these different methods were compared using simulation studies.

The nonlinear multicomponent analysis (NLMCA) technique is one of the two-flux evaluation methods for reflection spectra. For the samples of organic tissues with either finite or infinite thickness or even for the samples with light path distribution, it has been shown in Hoffmann et al. (1982) that, under certain conditions on light scattering within the tissues, the natural logorism of the ratio between the reflected light intensity to the incident beam intensity can be related to the total absorption spectra by a function with mild nonlinearity. Consequently, a linear rational function can be used to approximate the inverse of this mild nonlinearity and an iterative nonlinear multicomponent analysis algorithm can then be applied to estimate the parameters of this model from the observed reflection spectra and the spectra of individual components associated with hemoglobin, myoglobin, and cytochromes, etc. The results obtained is not only a model by which the reflection spectra can be evaluated but also the model parameters can represent the concentrations of associated components and the kinetics of the parameters reflect the oxygen supply and metabolism of these components in the involved organism.

In this report, the derivation of the relation between the reflection and absorption spectra based upon Kubelka-Munk theory is reviewed to introduce the foundation of the NLMCA technique. Then, the procedures of the iterative NLMCA algorithm are described and simulation studies are performed on examples including the model based on Kubelka-Munk theory for a semi-infinite plane homogeneous medium. The results indicate that the iterative NLMCA algorithm generally works well after a minor modification but is sensible to modelling errors due to invalid assumptions on the scattering properties of samples. A direct algorithm based on linear least squares is then suggested to deal with the same problem and simulation studies are performed to make a comparision with the iterative algorithm, which demonstrate better robust properties of the alternative strategy.

2. The Relation between the Reflection and Absorption Spectra

2.1 Kubelka-Munk theory

According to the Kubelka-Munk (K-M) theory (1931), for a layer of organic tissues with thickness d and under light illumination, the reflection spectra R, which is the ratio of reflected light intensity I to the incident beam intensity I_0, can be described by

$$R = \frac{I}{I_0} = \frac{\sinh(kd)}{\sinh(kd+y)} \tag{2.1}$$

where

$$k = \sqrt{a(a+2s)} \tag{2.2}$$

$$y = -\ln\left[\frac{(a+s-k)}{s}\right] \tag{2.3}$$

and a and s are referred to as the K-M absorption and scattering coefficients respectively. a and s are generally functions of the wavelength λ of the incident light, i.e.,

$$a = a(\lambda)$$

$$s = s(\lambda)$$

In the case of infinite thickness ($d \to \infty$),

$$R = R_\infty = \lim_{d\to\infty} \frac{e^{kd} + e^{-kd}}{e^{kd+y} + e^{-(kd+y)}} = \lim_{d\to\infty} \frac{e^{kd}}{e^{kd+y}} = e^{-y} = \frac{(a+s-k)}{s} \tag{2.4}$$

Substituting k into (2.4) yields

$$R_\infty = \frac{[a+s-\sqrt{a(a+2s)}]}{s} \tag{2.5}$$

which can be rewritten, after some manipulations, as

$$\frac{a(\lambda)}{s(\lambda)} = \frac{(1-R_\infty)^2}{2R_\infty} = f(R_\infty) \tag{2.6}$$

to yield a relationship between the reflection spectra R_∞, the absorption $a(\lambda)$ and the light scattering coefficient $s(\lambda)$, and $f(.)$ is called Kubelka-Munk function (Heinrich et al. 1981). Notice that for $0 < R_\infty < 1$, $f(R_\infty)$ is a monotonically decreasing function. In practice R_∞ always lies in the interval (0,1).

2.2 Lubbers Model

Heinrich and Lubbers et al. (1981) decomposed $s(\lambda)$ into a large wavelength independent part s_0 and a small wavelemgth dependent part $s_1(\lambda)$ to give

$$s(\lambda) = s_0 + s_1(\lambda) \tag{2.7}$$

Substituting (2.7) into (2.6) yields

$$a(\lambda) = s_0 f(R_\infty) + s_1(\lambda) f(R_\infty) \tag{2.8}$$

The absorption coefficient $a(\lambda)$ is usually modelled as the sum of the absorption spectra of the components of hemoglobin, myoglobin, and cytochrome, i.e.,

$$a(\lambda) = \sum_i c_i a_i(\lambda) = s_0 f(R_\infty) + s_1(\lambda) f(R_\infty) \tag{2.9}$$

where $a_i(\lambda)$ denotes the spectrum of the ith component (e.g., pure hemoglobin, myoglobin, or cytochrom) and c_i is the concentration of the corresponding component.

Since $s_1(\lambda)$ is assumed small, the last term in (2.9) is approximated by Heinrich et al. (1981) as

$$s_1(\lambda) f(R_\infty) = c_s \lambda \tag{2.10}$$

where c_s is a small constant. Substituting (2.10) into (2.9) gives

$$\sum_i c_i a_i(\lambda) - c_s \lambda = s_0 f(R_\infty) \tag{2.11}$$

Because $f(.)$ is a monotonic function for $0 < R_\infty < 1$, equation (2.11) defines a one-to-one relationship between $\sum_i c_i a_i(\lambda) - c_s \lambda$ and R_∞ for $0 < R_\infty < 1$.

Under a particular illumination of wavelength λ, $a_i(\lambda)$ are given by the book spectra. If $f(\cdot)$ is as defined in equation (2.6), one could estimate c_i and c_s up to a scalar. By noting that R_∞ is related to the ocular density (OD) function $y(\lambda)$ as

$$R_\infty = e^{-y(\lambda)}$$

which is also a monotonically decreasing function, equation (2.11) can be written as

$$\sum c_i a_i - c_s \lambda = s_0 f(e^{-y(\lambda)}) = g(y(\lambda)) \tag{2.12}$$

Clearly $g(.)$ is a monotonic function, therefore the inverse of this function exists. Using this property, Lubbers et al. (1981) attempted to extend the K-M function to a more general case by introducing another function $H(\cdot)$ such that

$$H^{-1}(\cdot) = g(\cdot)$$

Then equation (2.12) becomes

$$\sum c_i a_i - c_s \lambda = H^{-1}(y(\lambda)) \tag{2.13}$$

or

$$y(\lambda) = H\left(\sum c_i a_i - c_s \lambda\right) \tag{2.14}$$

It is therefore possible to explore a range of nonlinear functions $H(\cdot)$ which could be used as an approximation to the relationship between book spectra and $y(\lambda)$.

Heinrich et al. (1981) and Hoffmann et al. (1984) further assumed that $g(.) = H^{-1}(.)$ is a function with only mild nonlinearity and can therefore be sufficiently well approximated by a hyperbola as

$$g(y) = H^{-1}(y) = \frac{\alpha y(\lambda) + \beta}{\gamma y(\lambda) + 1} \tag{2.15}$$

where α, β, and γ are constants. Consequently, equation (2.14) can be written as

$$\sum_i c_i a_i(\lambda) - c_s \lambda = \frac{\alpha y(\lambda) + \beta}{\gamma y(\lambda) + 1} \tag{2.16}$$

and a nonlinear multicomponent analysis (NLMCA) algorithm can be applied to (2.16) to estimate the parameters α, β, γ, c_i, and c_s based on the measurement $y(\lambda)$ and the book spectra $a_i(\lambda)$. We refer to equation (2.16) as the Lubbers' Model.

Once the above parameters are estimated, the extent to which $y(\lambda)$ is approximated by the estimate $\hat{y}(\lambda)$ can be evaluated using the error (residue) signal

$$e_1(\lambda) = y(\lambda) - \hat{y}(\lambda) = y(\lambda) - \hat{H}\left[\sum_i \hat{c}_i a_i(\lambda) - \hat{c}_s \lambda\right] \tag{2.20}$$

Alternatively, the following residue signal

$$e_2(\lambda) = \hat{H}^{-1}(\hat{y}) - \hat{H}^{-1}(y) = \sum_i \hat{c}_i a_i(\lambda) - \hat{c}_s \lambda - \frac{\hat{\alpha} y(\lambda) + \hat{\beta}}{\hat{\gamma} y(\lambda) + 1} \tag{2.21}$$

can be estimated.

3. Simulation Studies of the NLMCA Technique for Reflection Spectra

3.1 The NLMCA Technique

The NLMCA algorithm used by Hoffman (1984) computes the parameters of equation (2.16) iteratively as follows.

(1) Set $\alpha = \alpha^{(1)} = 1$, $\beta = \beta^{(1)} = 0, \gamma = \gamma^{(1)} = 0$, use the OD $y(\lambda)$ and apply the linear least squares algorithm to equation (2.16) to estimate c_i and c_s. The results are denoted as $\hat{c}_i^{(1)}$, $\hat{c}_s^{(1)}$.

(2) Based on the estimation model

$$\sum_i \hat{c}_i^{(1)} a_i(\lambda) - \hat{c}_s^{(1)} \lambda = \frac{\alpha y(\lambda) + \beta}{\gamma y(\lambda) + 1} \tag{3.1}$$

a nonlinear least squares procedure is used to estimate α, β, and γ to yield the estimates $\hat{\alpha}^{(2)}$, $\hat{\beta}^{(2)}$, and $\hat{\gamma}^{(2)}$.

(3) From the estimation model

$$\sum_i c_i a_i(\lambda) - c_s\lambda = \frac{\hat{\alpha}^{(2)} y(\lambda) + \hat{\beta}^{(2)}}{\hat{\gamma}^{(2)} y(\lambda) + 1} \tag{3.2}$$

estimate c_i and c_s by a linear least squares. Denote the estimates as $\hat{c}_i^{(2)}$, $\hat{c}_s^{(2)}$ and repeat the iteration until the parameters converge, or a pre-specified number of iterations is reached.

It is worth pointing out that the parameters c_i, c_s, α, and β can only be estimated up to an arbitrary scalar. This is evident by noting that multiplying a constant ρ on both sides of the Lubbers model yields

$$\sum \rho\ c_i a_i(\lambda) - \rho\ c_s\lambda = \frac{\rho\alpha y(\lambda) + \rho\ \beta}{\gamma\ y + 1}$$

and the equation holds whatever value this constant takes.

3.2 Simulation results

3.2.1 Simulation 1

- Data generation:

The OD $y(\lambda)$ was generated using the K-M theory as

$$y(\lambda) = -\ln\left[\frac{a(\lambda) + s(\lambda) - k(\lambda)}{s(\lambda)}\right] \tag{3.3}$$

where

$$k(\lambda) = \sqrt{a(\lambda)(a(\lambda) + 2s(\lambda))}$$

and assuming the scattering is a linear function of wavelength such that

$$s(\lambda) = s_0 + s_1\lambda$$

The absorption term is given by

$$a(\lambda) = \sum_{i=1}^{4} c_i a_i(\lambda)$$

where $a_i(\lambda)$, $i = 1,2,3,4$, and λ are book spectra and wavelength in the range $500 - 700nm$ respectively, and c_i, $i = 1,2,3,4$, are concentration coefficients chosen arbitrarily as

$$c_1 = 0.57v,\ c_2 = 0.43v,\ c_3 = 0.35v,\ c_4 = 0.21v$$

with $v = 0.01$.

One objective of this simulation is to test the robustness of the NLMCA w.r.t. the assumption of s_1 being small. Thus, we chosen s_0=312 v and s_1=0, 0.018 v, 0.18 v, and 1.8 v, respectively, to produce four sets of data for $y(\lambda)$ using equation (3.3).

• Parameter estimation:

The objective is to model the data $y(\lambda)$ generated above using Lubbers model equation (2.16) in order to estimate the concentration coefficients c_i. Note that these coefficients can only be estimated up to a scalar. Thus comparison between the true and estimated parameters can only be made in terms of ratios.

By applying the NLMCA iterative algorithm directly to each of the four data sets, the estimates for concentrations c_i are shown in Table 1 and Figs.1,2,3, and 4..

The parameter estimates thus obtained do not converge in the process of iterative computations even when $s_1 = 0$ and are therefore unsatisfactory. This is believed to be due to the unstable property of the iterative process caused by the considerable difference between the real and applied estimation models.

To deal with this problem, the Lubbers model (2.16) is slightly modified as

$$\sum_i c_i a_i(\lambda) - c_s\lambda + \eta = \frac{\alpha y(\lambda) + \beta}{\gamma y(\lambda) + 1} \tag{3.4}$$

Notice that equation (3.4) is essentially the same as (2.16) because shifting η to the right hand side and combining η and the fraction associated with α, β, γ into one term yields an equation which is exactly the same as (2.16) in structure. However, the iterative computations using (3.4) are based on a relatively general model which contains a constant term when setting $\alpha = \alpha^{(1)} = 1$, $\beta = \beta^{(1)} = 0, \gamma = \gamma^{(1)} = 0$ to estimate c_i and c_s. This could produce relatively reliable estimation results.

The simulation results using this modified model are shown in Table 2 and Figs. 5,6,7, and 8 and the following points can be observed from these results..

(1) All estimates using modified Lubbers method seem to converge after about 20 iterations.

(2) The errors associated with estimates of c_i/c_1 increase as s_1 increases. Even at $s_1 = 0$ the estimation errors are significant.

• Conclusions from the simulation

The original NLMCA iterative algorithm needs to be modified in order to overcome the divergence problem with the original Lubbers model.

The derivation of the NLMCA iterative algorithm is based on K-M theory and the following key assumptions:

(i) The scattering coefficients can be approximated by $s(\lambda) = s_0 + s_1(\lambda)$ for $s_1(\lambda)$ being very small.

(ii) The term $s_1 f(R_\infty)$ can be approximated by $c_s\lambda$. The implication of this assumption is that $s_1 f(R_\infty)$ can be approximated as proportional to the wavelength λ.

(iii) The nonlinearity in $f(.)$ is mild and the term $f(e^{-y})$ can be approximated by

$$\frac{\alpha y + \beta}{\gamma y + 1}$$

The above simulation results showed that even by setting $s_1(\lambda) \equiv 0$ Lubbers model yield biased estimates for concentrations. This suggests that the assumption (iii) is not very good as far as the K-M function is concerned. It also implies that Lubbers method is sensitive to modelling errors. The second assumption above is also questionable because $f(.)$ is unknown and is to be estimated. In fact it could be argued from the simulation above that a better approximation to $s_1 f(R_\infty)$ could be $c_{s1} + c_{s2}\lambda$!

Table 1. Parameter estimates using the original Lubbers model where the output data are produced using $y=-\ln R_\infty = -\ln\frac{a+s-k}{s}$ (Results at the 1500th step iteration)

		$\frac{c_2}{c_1}$	$\frac{c_3}{c_1}$	$\frac{c_4}{c_1}$	$\frac{c_s}{c_1}$
True $\frac{c_i}{c_1}$		0.7544	0.6140	0.3684	
Parameter Estimates and Relative Errors under Different Cases of s_1	s_1=0 v	0.73770	0.86802	0.51211	-0.01245
	(Relative Error)	(2.21%)	(-41.36%)	(-39.00%)	
	s_1=0.018 v	0.73678	0.88436	0.52183	-0.01221
	(Relative Error)	(2.33%)	(-44.02%)	(-41.64%)	
	s_1=0.18 v	0.73182	1.00616	0.58879	-0.01094
	(Relative Error)	(2.99%)	(-63.86%)	(-59.81%)	
	s_1=1.8 v	0.72685	1.37663	0.75927	-0.00962
	(Relative Error)	(3.64%)	(-124.19%)	(-106.09%)	

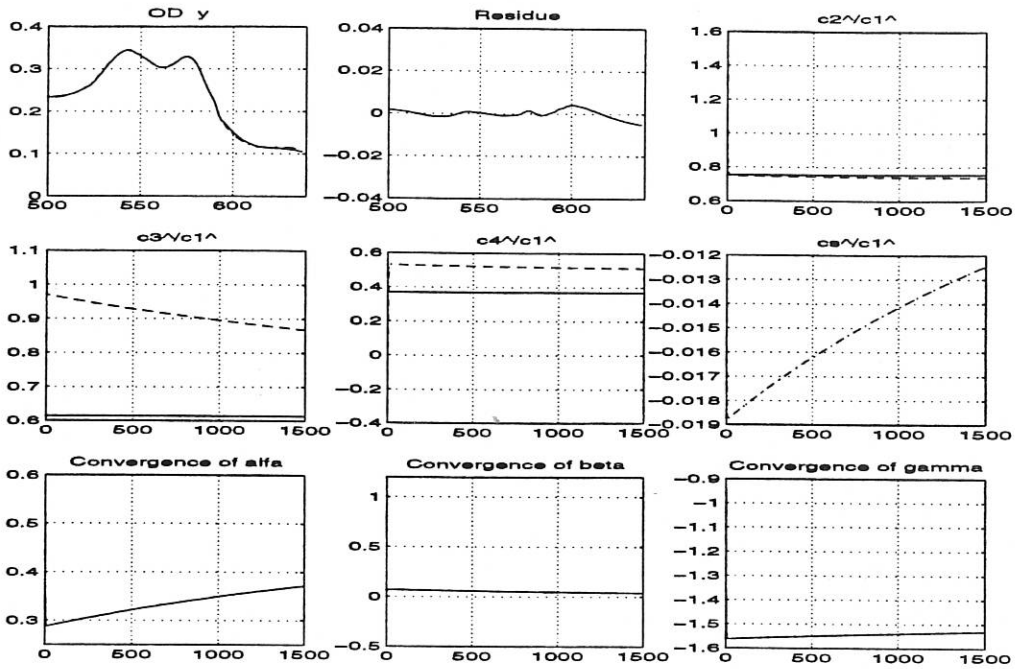

Fig. 1. Simulation results for the original Lubbers method in the case of $s_1 = 0$

Generated OD y is solid and the estimated OD $\hat{y}$ dashed. Residue $e_1(\lambda)$ is defined by equation (2.20). For the estimates of c_i/c_1, solid lines show the real values and dotted lines the estimates. For the results of OD and residue, the horizontal axis represents the wave length. For others, the horizontal axis represents the times of iteration.

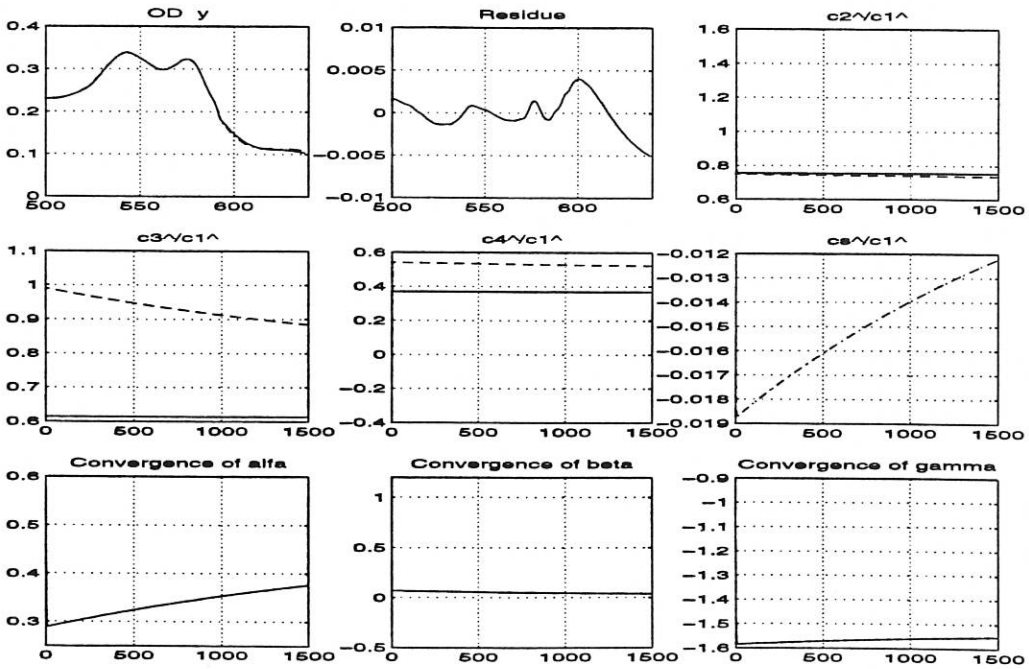

Fig. 2. Simulation results for the original Lubbers method in the case of $s_1 = 0.018v$

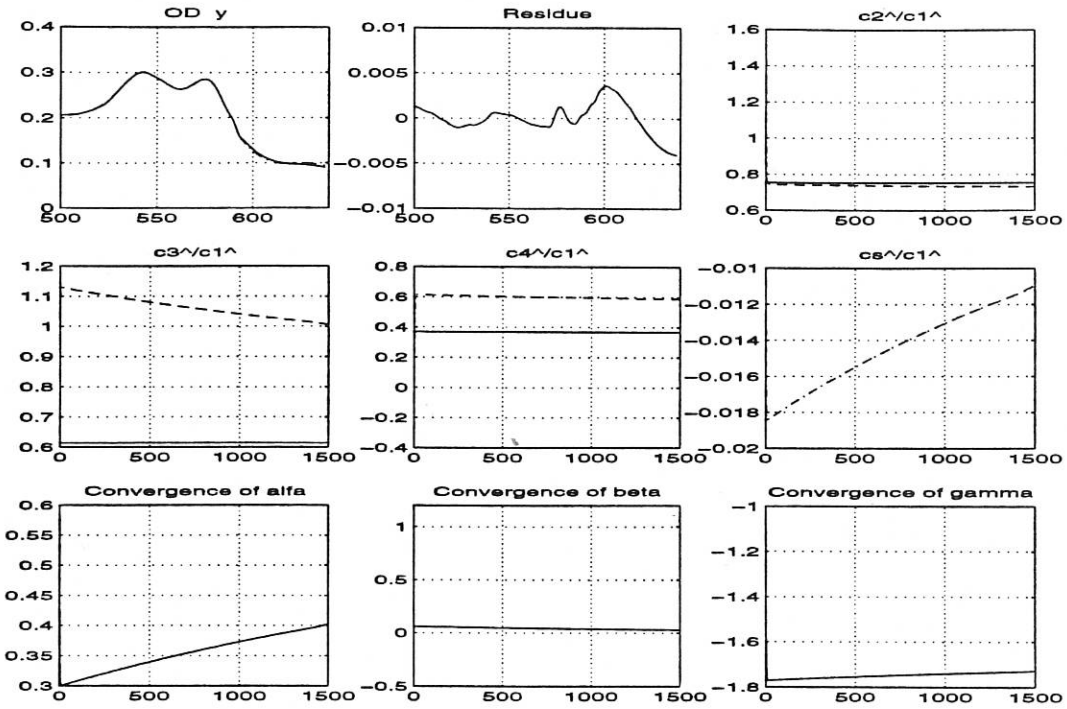

Fig.3. Simulation results for the original Lubbers method in the case of $s_1 = 0.18v$

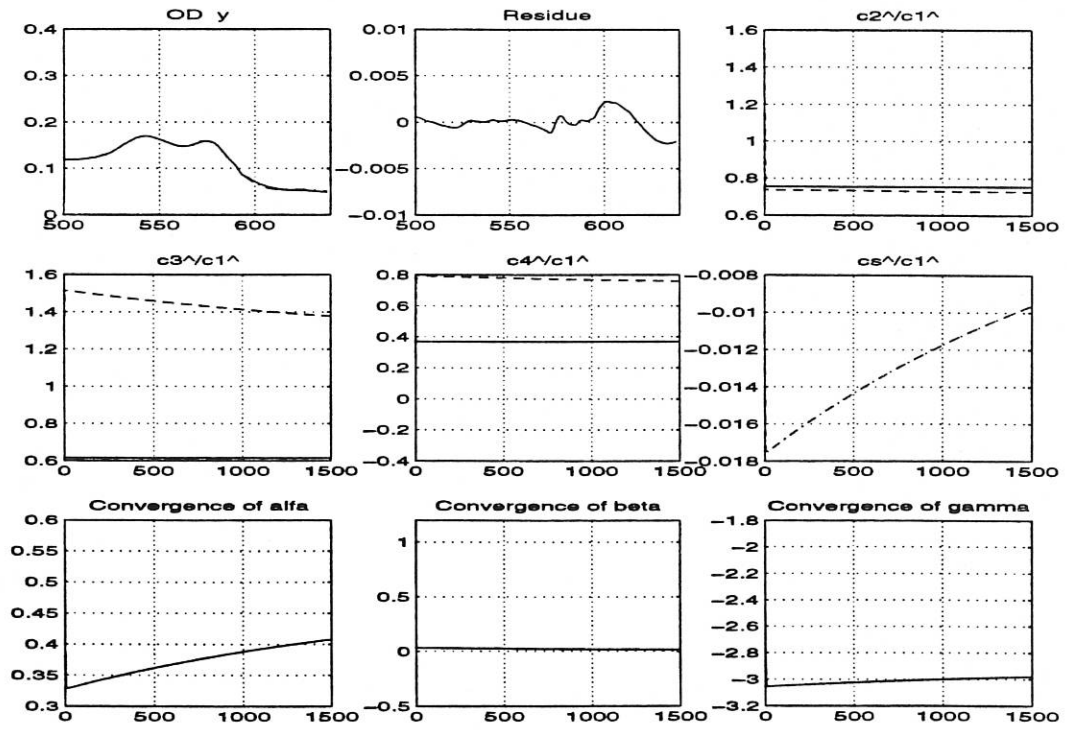

Fig. 4. Simulation results for the original Lubbers method in the case of $s_1 = 1.8v$

Table 2. Parameter estimates using the modified Lubbers model where the output data are produced using $y = -\ln R_\infty = -\ln \frac{a+s-k}{s}$

		$\frac{c_2}{c_1}$	$\frac{c_3}{c_1}$	$\frac{c_4}{c_1}$	$\frac{c_s}{c_1}$
True $\frac{c_i}{c_1}$		0.7544	0.6140	0.3684	
Parameter Estimates and Relative Errors under Different Cases of s1	s1=0 v	0.69698	0.50520	0.44859	0.01026
	(Relative Error)	(7.60%)	(17.72%)	(-21.76%)	
	s1=0.018 v	0.69661	0.52026	0.45670	0.01051
	(Relative Error)	(7.65%)	(15.27%)	(-23.96%)	
	s1=0.18 v	0.69427	0.62360	0.51089	0.01245
	(Relative Error)	(7.96%)	(-1.55%)	(-38.67%)	
	s1=1.8 v	0.69067	0.87842	0.63210	0.01901
	(Relative Error)	(8.44%)	(-43.05%)	(-71.57%)	

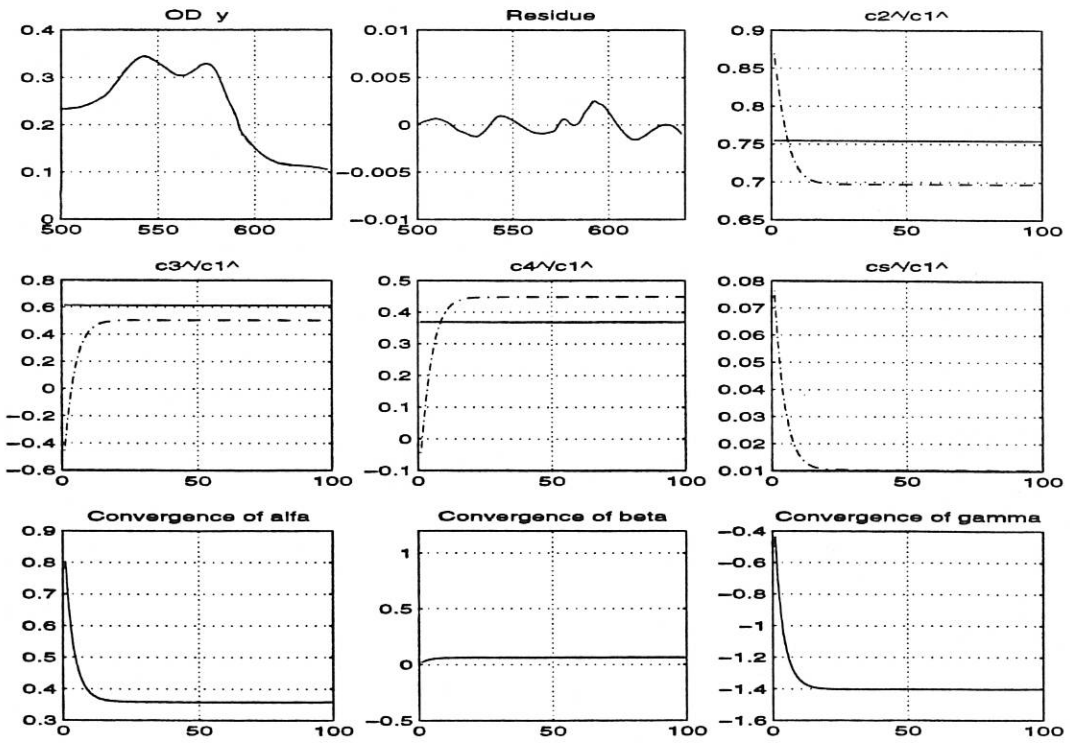

Fig.5. Simulation results for the modified Lubbers method in the case of $s_1 = 0$ v

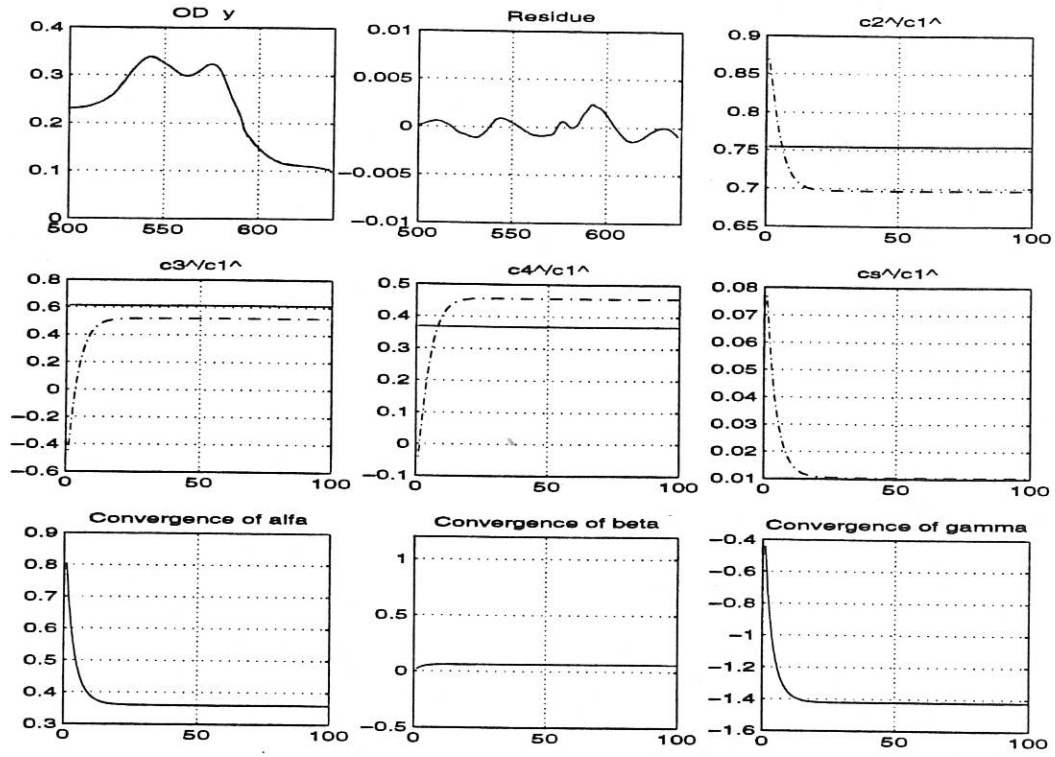

Fig.6. Simulation results for the modified Lubbers method in the case of $s_1 = 0.018\,v$

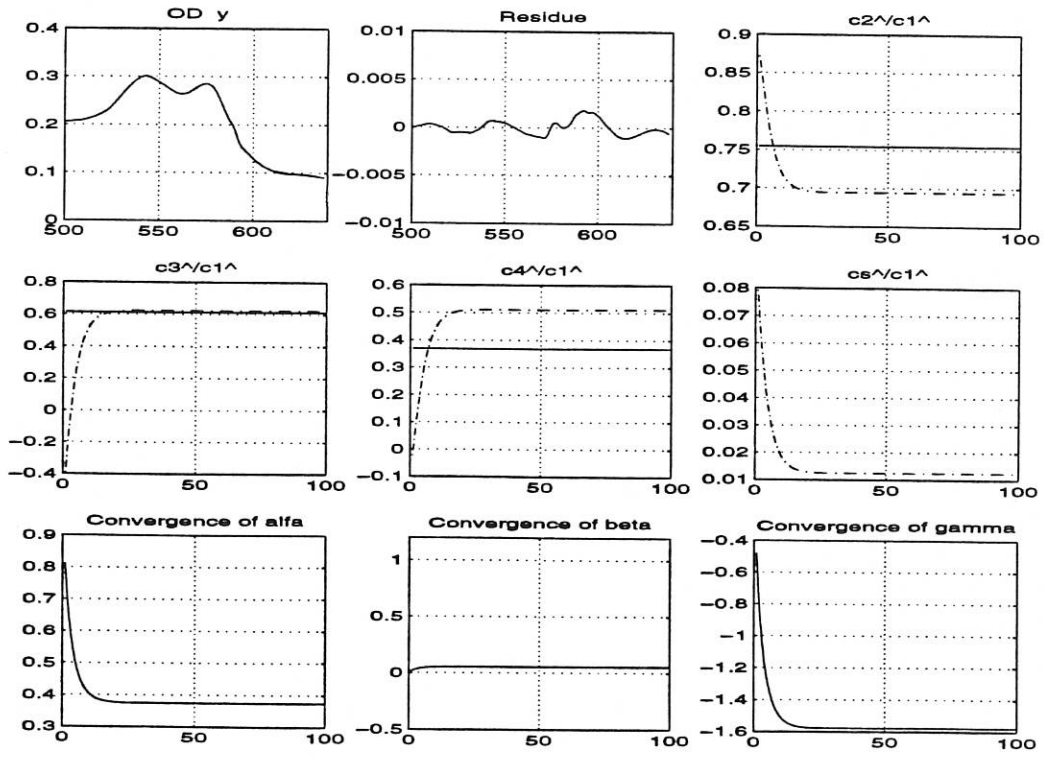

Fig.7. Simulation results for the modified Lubbers method in the case of $s_1 = 0.18\,v$

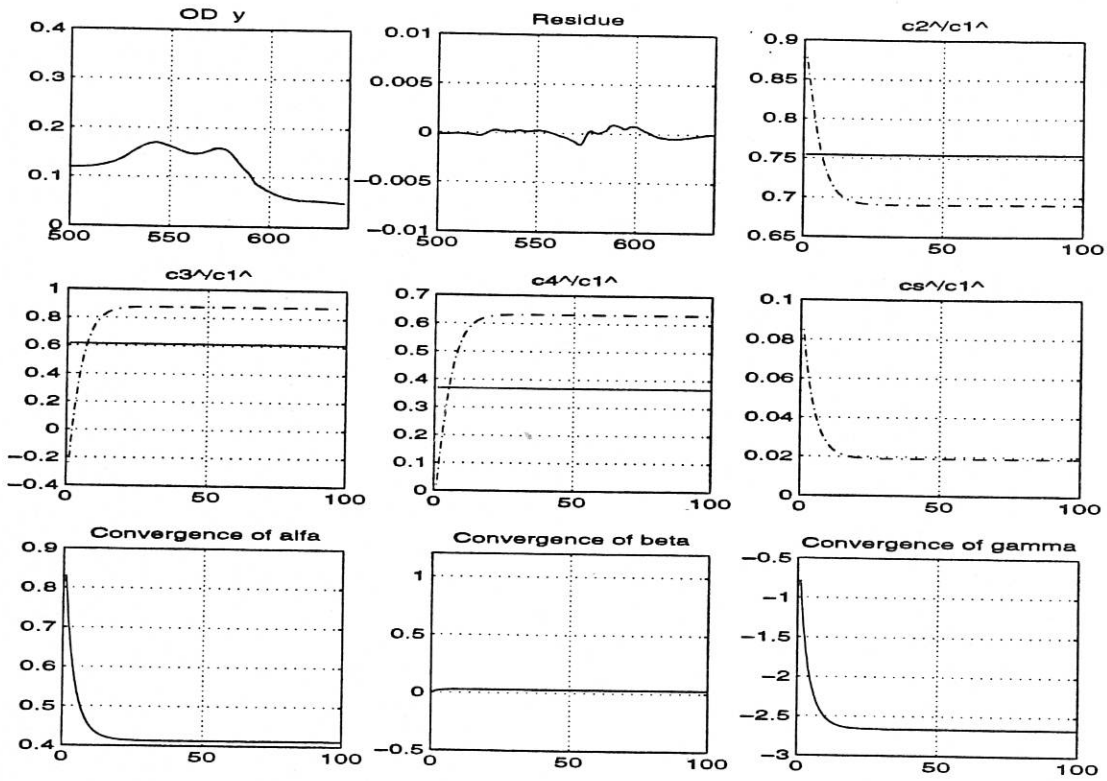

Fig.8. Simulation results for the modified Lubbers method in the case of $s_1 = 1.8\,v$

3.2.2. Simulation 2

• Data generation:

In many cases, the Beer-Lambert Law is assumed in analysing the relationship between the reflection and absorbstion spectra. Based upon this law,

$$R = e^{-v[a(\lambda)+s(\lambda)]} \tag{3.5}$$

Thus, in this set of simulation, data $y(\lambda)$ was generated using

$$y(\lambda) = -\ln(R) = v[a(\lambda) + s_0 + s_1(\lambda)] = v\left[\sum_i c_i a_i(\lambda) - c_s\lambda + s_0\right] \tag{3.6}$$

where it is assumed that $s_1(\lambda) = -c_s\lambda$, which is similar to the approximation given in (2.10). Clearly, (3.6) is a special case of (3.4) with $\alpha = 1$, $\beta = \gamma = 0$ and the NLMCA technique should, therefore, apply.

The parameters are chosen as follows.

v=0.01, $c_1 = 0.57$, $c_2 = 0.43$, $c_3 = 0.35$, $c_4 = 0.21$, $s_o = 312$.

a_i and λ are the same as above and four different values of c_s=0, 0.018, 0.18, and 1.8 are also considered.

• Parameter estimation:

Modified Lubbers model (3.4) is now used to estimate the concentration coefficients. Table 3 and Figs. 9, 10, 11, and 12 show the results. They are clearly very satisfactory and irrespective of different values of s_1. This is because the model structure is always consistent with the real data generation structure.

• Conclusions from the simulation

If the real data $y(\lambda)$ is generated by the Bear-Lambert law, parameter estimates obtained using the modified Lubbers model are very close to the real ones for all s_1 due to the fact that the model structure and the data generation structure are identifical.

Table 3. Parameter estimates using the modified Lubbers model where the output data are produced by $y = -\ln R_\infty = -v[a(\lambda) + s]$

		$\frac{c_2}{c_1}$	$\frac{c_3}{c_1}$	$\frac{c_4}{c_1}$	$\frac{c_s}{c_1}$
True $\frac{c_i}{c_1}$		0.7544	0.6140	0.3684	
Parameter Estimates and Relative Errors under different Cases of s1	s1=0	0.7544	0.6140	0.3684	0
	(Relative Error)	(0%)	(0%)	(0%)	
	s1=0.018	0.7544	0.6140	0.3684	-0.03157
	(Relative Error)	(0%)	(0%)	(0%)	
	s1=0.18	0.7544	0.6140	0.3684	-0.31578
	(Relative Error)	(0%)	(0%)	(0%)	
	s1=1.8	0.7544	0.6140	0.3684	-3.15789
	(Relative Error)	(0%)	(0%)	(0%)	

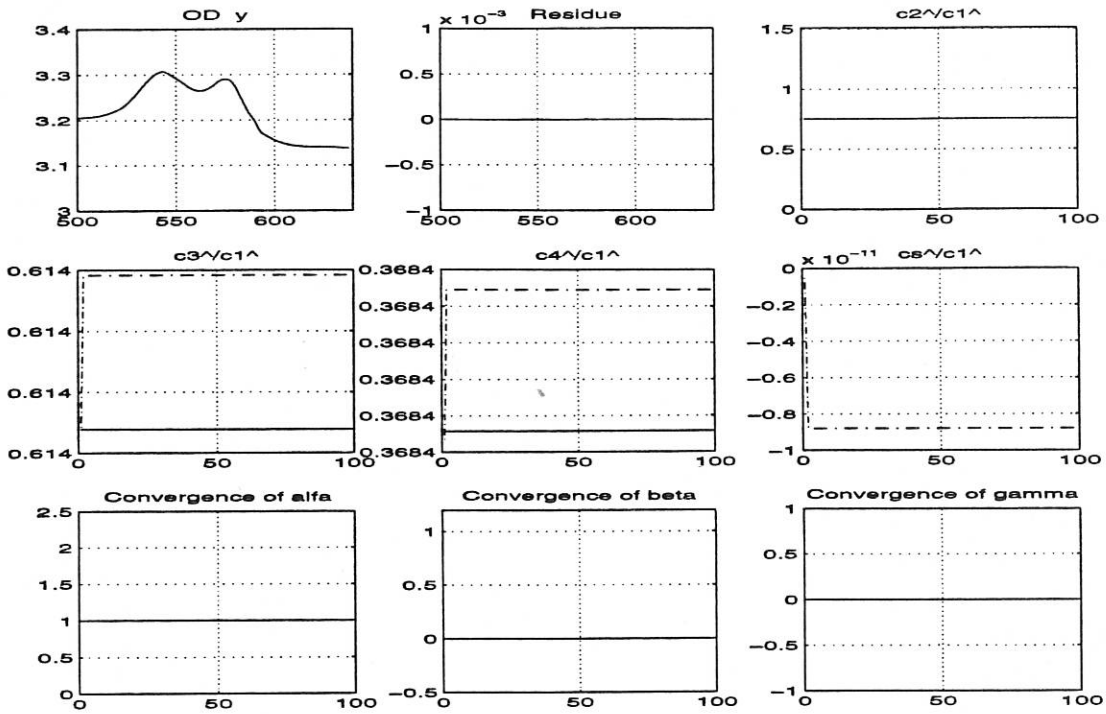

Fig.9. Simulation results for the modified Lubbers method in the case of $s_1 = 0$ and when y is generated using Beer-Lambert Law

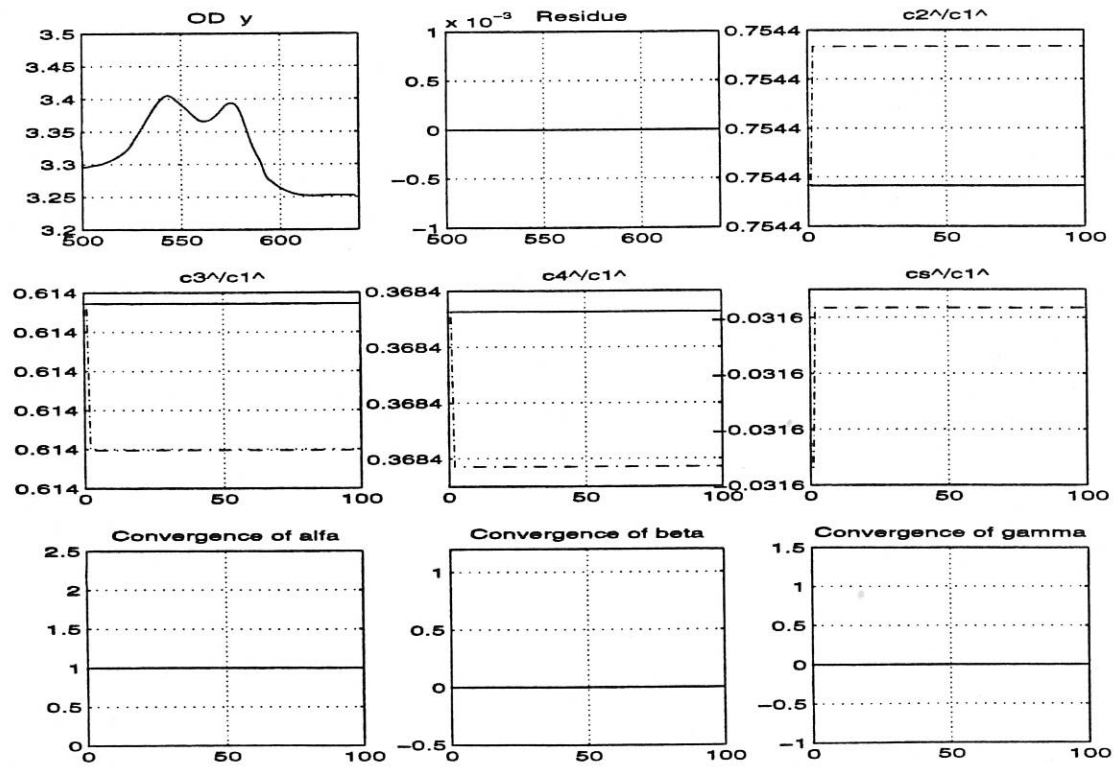

Fig.10. Simulation results for the modified Lubbers method in the case of $s_1 = 0.018$ and when y is generated using Beer-Lambert Law

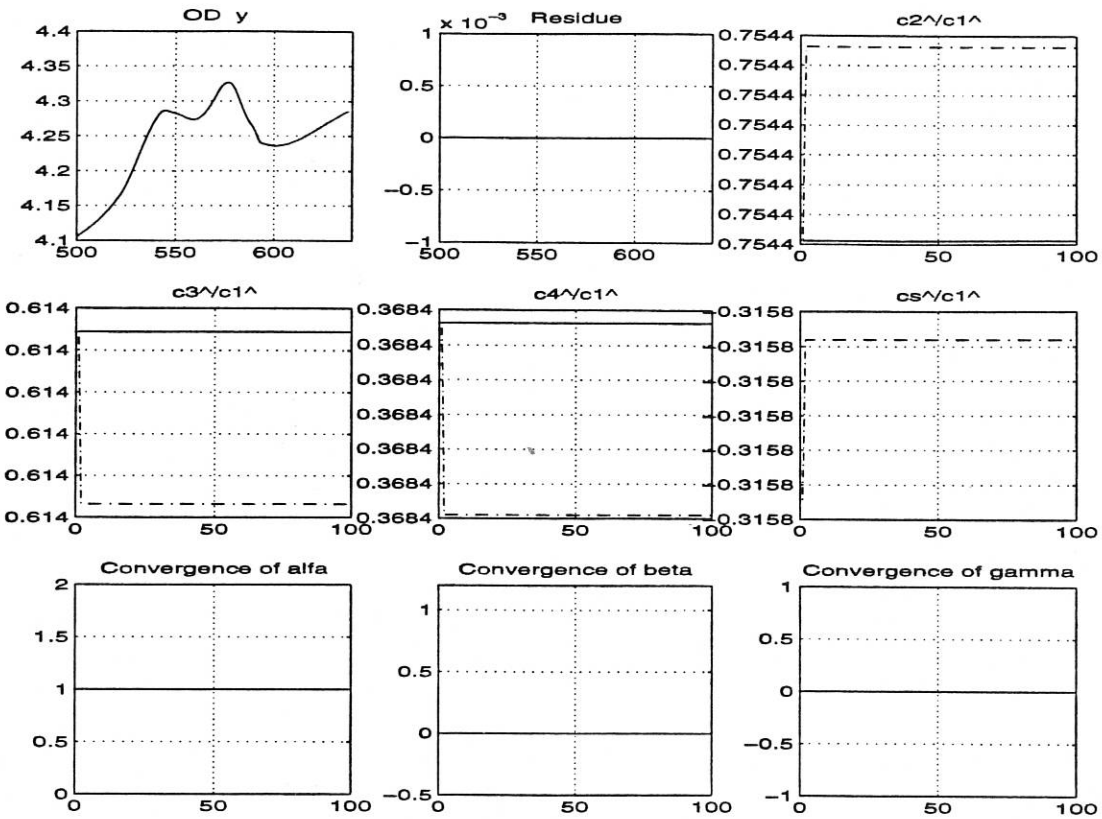

Fig.11. Simulation results for the modified Lubbers method in the case of $s_1 = 0.18$ and when y is generated using Beer-Lambert Law

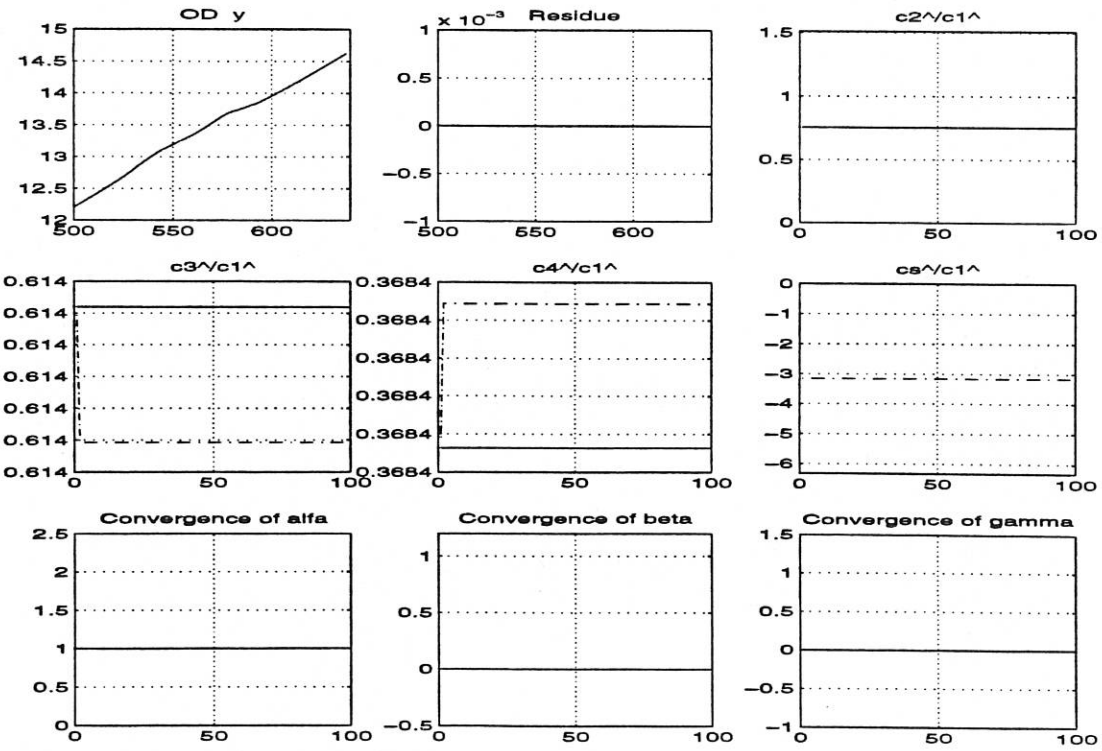

Fig.12. Simulation results for the modified Lubbers method in the case of $s_1 = 1.8$ and when y is generated using Beer-Lambert Law

4. A Linear Least Squares Based Direct Algorithm (Ratio Method)

The NLMCA iterative algorithm for reflection spectra analysis is an iterative method for obtaining solutions to nonlinear least squares optimisation problems. The disadvantage with this algorithm is the problem associated with the iterative computation procedure which involves an important issue of convergence. In order to circumvent this problem, a linear least squares based direct algorithm is proposed below to directly estimate the parameters associated with α, β, γ, c_i, and c_s based on the original model structure (2.16), thus no iteration is necessary.

Rewrite equation (2.16) as

$$\begin{aligned} y(\lambda) &= \sum_i \frac{c_i\gamma}{\alpha} a_i(\lambda)y(\lambda) + \sum_i \frac{c_i}{\alpha} a_i(\lambda) - \frac{c_s\gamma}{\alpha} y(\lambda)\lambda - \frac{c_s}{\alpha}\lambda - \frac{\beta}{\alpha} \\ &= \sum_i p_i a_i(\lambda)y(\lambda) + \sum_i q_i a_i(\lambda) - d_1 y(\lambda)\lambda - d_2\lambda - d_3 \end{aligned} \tag{4.1}$$

where $p_i = \frac{c_i\gamma}{\alpha}$, $q_i = \frac{c_i}{\alpha}$, $d_1 = \frac{c_s\gamma}{\alpha}$, $d_2 = \frac{c_s}{\alpha}$, $d_3 = \frac{\beta}{\alpha}$, a linear least squares algorithm can be applied directly to model (4.1) to obtain the estimates $\hat{p}_i$, $\hat{q}_i$, $\hat{d}_1$, $\hat{d}_2$, $\hat{d}_3$ for the parameters p_i, q_i, d_1, d_2, d_3. The estimates for the ratios of $\frac{c_i}{c_1}$ can then be obtained as

$$\left(\frac{c_i}{c_1}\right)^{\wedge} = \frac{\hat{q}_i}{\hat{q}_1} \text{ or } \frac{\hat{p}_i}{\hat{p}_1} \tag{4.2}$$

and $\frac{c_s}{c_1}$ from $\frac{\hat{d}_1}{\hat{p}_1}$. The OD can be evaluated using the obtained parameters estimates as

$$\hat{y}(\lambda) = \frac{\sum_i \hat{q}_i a_i(\lambda) - \hat{d}_2\lambda - \hat{d}_3}{1 - \sum_i \hat{p}_i a_i(\lambda) + \hat{p}_i\lambda} \tag{4.3}$$

Simulation 1:

- Data generation:

  The same as in Section 3.2.1.

- Parameter estimation:

The results for the estimated c_i/c_1 are shown in Table 4, indicating that similar results can be obtained for all cases of s_1 but considerable biases of estimation exist in the obtained results. Figs.13, 14, 15, and 16 show the residues of the obtained models in the different cases of s_1, which are evaluated as

$$y(\lambda) - \hat{y}(\lambda)$$

where $\hat{y}(\lambda)$ is defined by equation (4.3).

• Conclusions from the simulation

The simulation demonstrates that this alternative strategy yields estimates which are rather robust over a wide a range of s_1. However the estimates are still significantly biased. The biases are believed to be caused by the errors of the model.

Table 4. Parameter estimates obtained by the ratio method where the output data are produced using $y = -\ln R_\infty = -\ln \frac{a+s-k}{s}$

		$\frac{c_2}{c_1}$	$\frac{c_3}{c_1}$	$\frac{c_4}{c_1}$	$\frac{c_s}{c_1}$
True $\frac{c_i}{c_1}$		0.7544	0.6140	0.3684	
Parameter estimates and Relative Errors under Different Cases of s1	s1=0 v	0.80428	0.69935	0.69267	0.02838
	(Relative Error)	(-6.61%)	(-13.89%)	(-88.01%)	
	s1=0.018 v	0.80384	0.69663	0.69323	0.02827
	(Relative Error)	(-6.55%)	(-13.45%)	(-88.16%)	
	s1=0.18 v	0.79893	0.67788	0.69838	0.02757
	(Relative Error)	(-5.90%)	(-10.39%)	(-89.56%)	
	s1=1.8 v	0.76434	0.63099	0.72669	0.02658
	(Relative Error)	(-1.32%)	(-2.76%)	(-97.24%)	

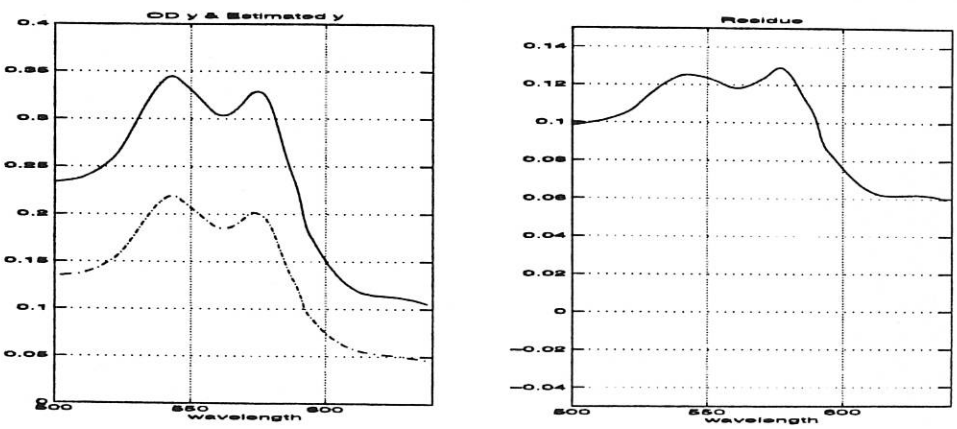

Fig. 13. Residue in the case of $s_1 = 0\ v$

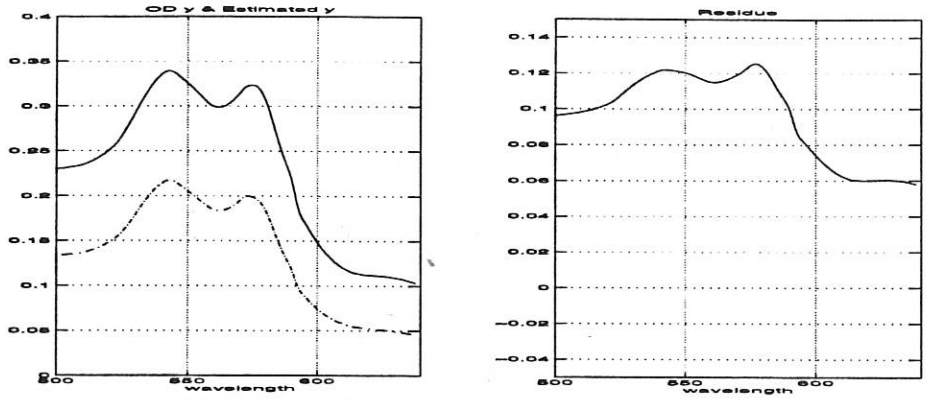

Fig. 14. Residue in the case of $s_1 = 0.018\ v$

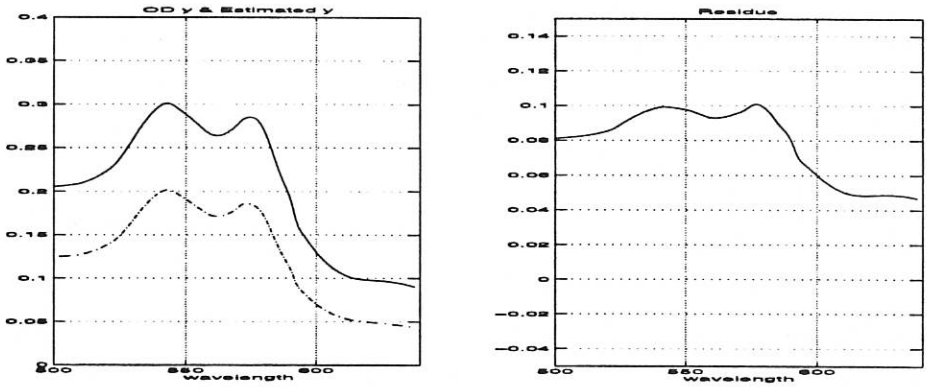

Fig. 15. Residue in the case of $s_1 = 0.18\ v$

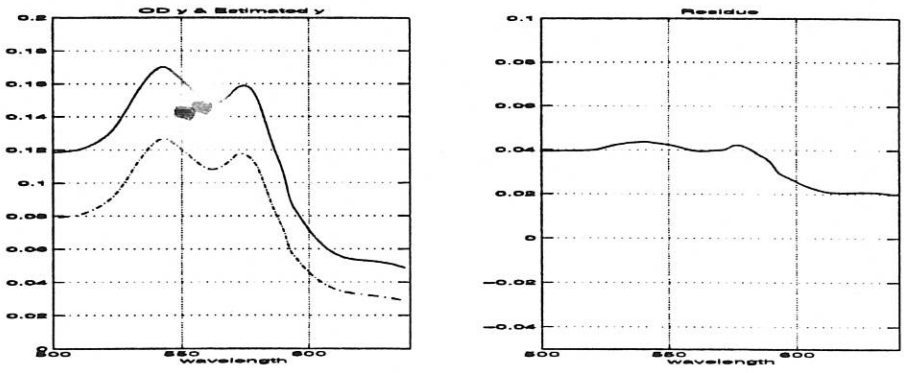

Fig. 16. Residue in the case of $s_1 = 1.8\ v$

Simulation 2

- Data generation:

  The same as in Section 3.2.2.

- Parameter estimation:

  Simulation studies for the direct least squares based method are performed to yield the estimation results for c_i given in Table 5 and corresponding model residues shown in Figs. 17, 18, 19, and 20. Clearly, satisfactory results are obtained in this case.

- Conclusions from the simulation

  Satisfactory parameter estimates can be obtained using the ratio method when the estimation model applied is consistent with the model by which the simulation data are generated.

Table 5. Parameter estimates obtained by the ratio method where the output data are produced using $y = -\ln R_\infty = -v[a(\lambda) + s]$

		$\frac{c_2}{c_1}$	$\frac{c_3}{c_1}$	$\frac{c_4}{c_1}$	$\frac{c_s}{c_1}$
True $\frac{c_i}{c_1}$		0.7544	0.6140	0.3684	
Parameter estimates and Relative Errors under Different Cases of s1	s1=0	0.7544	0.6140	0.3684	-0.003157
	(Relative Error)	(0%)	(0%)	(0%)	
	s1=0.018	0.7544	0.6140	0.3684	-0.031578
	(Relative Error)	(0%)	(0%)	(0%)	
	s1=0.18	0.7544	0.6140	0.3684	-0.31578
	(Relative Error)	(0%)	(0%)	(0%)	
	s1=1.8	0.7544	0.6140	0.3684	-3.1578
	(Relative Error)	(0%)	(0%)	(0%)	

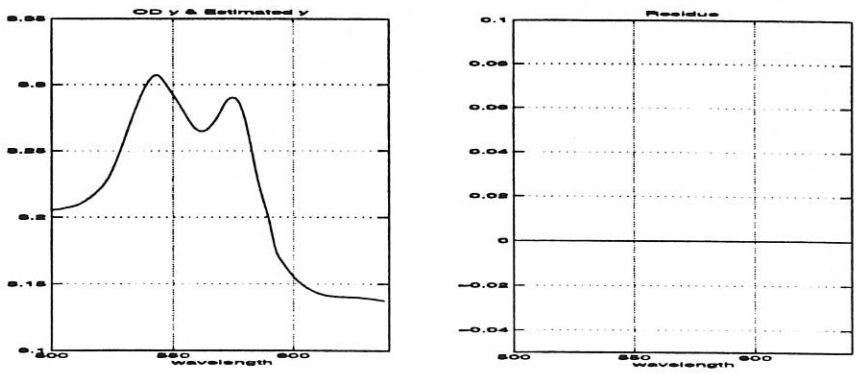

Fig. 17. Residue in the case of $s_1 = 0$ and when data are produced using $y = -\ln R_\infty = -v[a(\lambda) + s]$

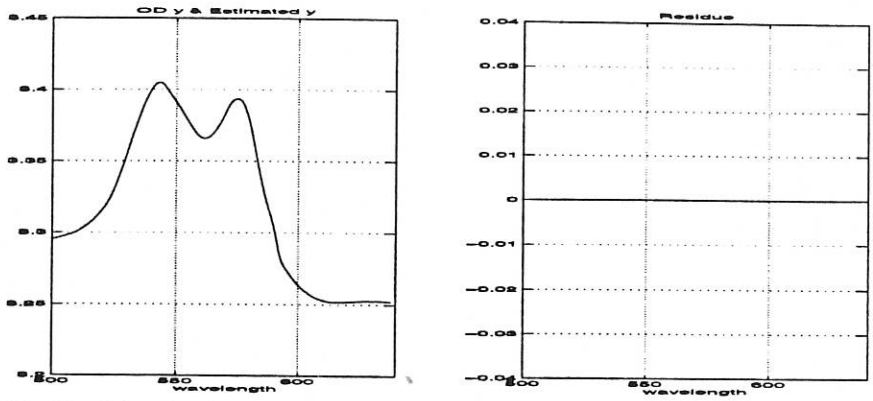

Fig.18. Residue in the case of $s_1 = 0.018$ and when data are produced using $y = -\ln R_\infty = -\nu[a(\lambda) + s]$

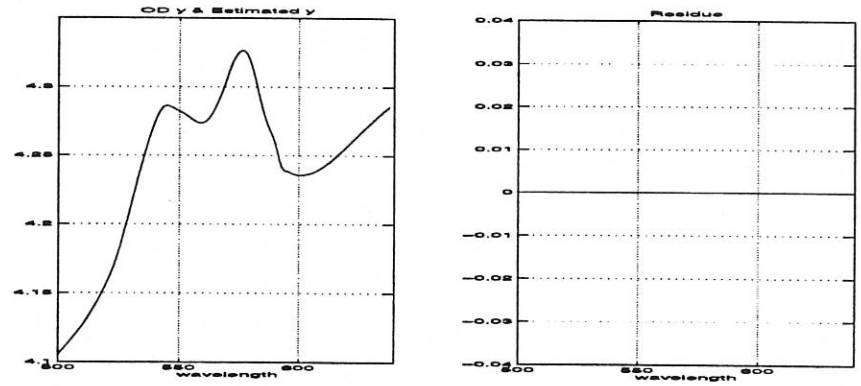

Fig.19. Residue in the case of $s_1 = 0.18$ and when data are produced using $y = -\ln R_\infty = -\nu[a(\lambda) + s]$

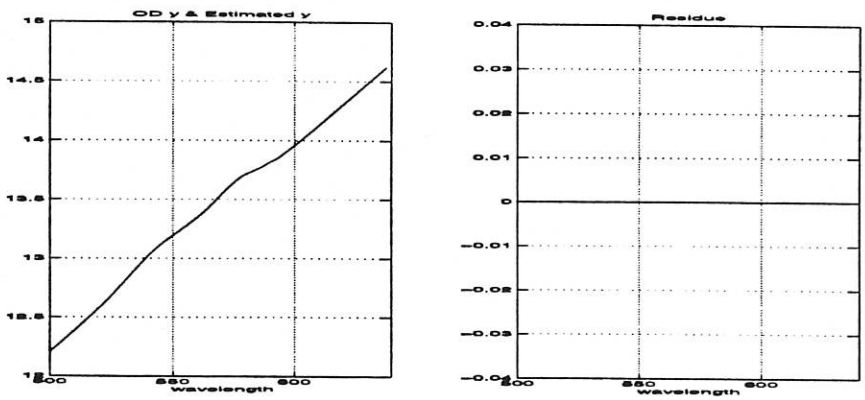

Fig.20. Residue in the case of $s_1 = 1.8$ and when data are produced using $y = -\ln R_\infty = -\nu[a(\lambda) + s]$

5. Simulation Using the Exact Kubelka-Munk Model

Instead of using Lubbers model which attempts to generalise the Kubelka-Munk model to cases with mild nonlinearities, the following set of simulation uses the Kubelka-Munk model for parameter estimation.

The Kubelka-Munk model is given by equation (2.6) as

$$\frac{a(\lambda)}{s(\lambda)} = \frac{(1-R_\infty)^2}{2R_\infty} = f(R_\infty)$$

which can be written as

$$\frac{\sum_i c_i a_i}{f(R_\infty)} = s_0 + s_1\lambda$$

Since the functional form of f is known, a least squares routine can be easily used to obtain the estimates for the concentration coefficients of the model.

Simulation 1

- Data generation:

$y(\lambda)$ is generated using the Kubelka-Munk model with other data and parameters the same as those in Section 3.2.1.

- Parameter estimation:

The parameter estimation results obtained using the least squares routine are given in Table 6 indicating that excellent parameter estimates are obtained.

- Conclusions from the simulation:

Least squares method works well for the Kubelka-Munk model when the data are generated using the same model as expected.

Simulation 2

- Data generation:

$y(\lambda)$ is generated using the Beer-Lambert law model with other data and parameters the same as those in Section 3.2.2.

- Parameter estimation:

The parameter estimation results obtained using the same least squares routine above are given in Table 7 indicating that the parameter estimates are very poor.

- Conclusions from the simulation:

Least squares method does not work if the estimation model applied is totally different from the real model.

6. Discussions

In this report, the NLMCA technique for reflection spectra is evaluated using simulation examples. It has been shown that the technique needs a minor modification and even so it yields biased estimates. The bias increases as the assumption about the scattering coefficient is more violated. A direct linear least squares based algorithm has been proposed which has been shown to be more effective in terms of robustness over the scattering coefficient but further investigation is required to resolve the problem of biased parameter estimates.

Table 6. Parameter estimates obtained when applying the pure Kubelka-Munk method where the output data are produced using

$$y = -\ln R_\infty = -\ln \frac{a+s-k}{s}$$

		$\frac{c_2}{c_1}$	$\frac{c_3}{c_1}$	$\frac{c_4}{c_1}$	$\frac{c_s}{c_1}$
True $\frac{c_i}{c_1}$		0.7544	0.6140	0.3684	
Parameter estimates and Relative Errors under Different Cases of sl	sl=0 v (Relative Error)	0.7544 (0%)	0.6140 (0%)	0.3684 (0%)	0
	sl=0.018 v (Relative Error)	0.7544 (0%)	0.6140 (0%)	0.3684 (0%)	0.03157
	sl=0.18 v (Relative Error)	0.7544 (0%)	0.6140 (0%)	0.3684 (0%)	0.315789
	sl=1.8 v (Relative Error)	0.7544 (0%)	0.6140 (0%)	0.3684 (0%)	3.15789

Table 7. Parameter estimates when applying the pure Kubelka-Munk method where the output data are produced using $y = -\ln R_\infty = -v[a(\lambda) + s]$

		$\frac{c_2}{c_1}$	$\frac{c_3}{c_1}$	$\frac{c_4}{c_1}$	$\frac{c_s}{c_1}$
True $\frac{c_i}{c_1}$		0.7544	0.6140	0.3684	
Parameter estimates and Relative Errors under Different Cases of s1	s1=0	15.57028	44.4371	-3.92722	-0.22781
	(Relative Error)	-----	-----	-----	
	s1=0.018	16.23947	45.95412	-3.99314	-0.21653
	(Relative Error)	------	------	------	
	s1=0.18	23.32767	60.70938	-4.42376	-0.13447
	(Relative Error)	--------	------	------	
	s1=1.8	-18.56905	-7.13678	-0.7384	1.11391
	(Relative Error)	--------	-------	-------	

REFERENCES

[1] Tobias Bonhoeffer and Amiram Grinvald, "Optical Imaging based on Intrinsic Signals: The Methodology"

[2] Wai-fung Cheong, Scott A. Prahl, and Ashley J. Welch, " A Review of the Optical Properties of Biological Tissues", IEEE Journal of Quantum Electronics. Vol. 26, No. 12, pp. 2166-2185, December 1990

[3] Kevin Farrell, "Analysis of the Interrelationships of Non-Nutrient Blood Flow, Oxygen Delivery, Oxygen Consumption, and the Ratio of Oxygen Delivery/Oxygen Consumption Based on a Mathematical Model of Non-Nutrient Blood Flow", Advances In Experimental Medicine and Biology Oxygen Transport To Tissue-IV, Vol.159, pp.569-577, 1981

[4] H.R.Figulla, J.Hoffmann and D.W. Lubbers, "Coronary Conductivity and Tissue Oxygenation as Measured by the Myoglobin O_2 Saturation and the Cytochrome AA_3 Redox State in the Langendorff Guinea Pig heart Preparation", Advances In Experimental Medicine and Biology Oxygen Transport To Tissue-IV, Vol.159, pp.579-585, 1981

[5] U.Heinrich, J.Hoffmann and D.W. Lubbers, "Quantitative Analysis of Reflection Spectra on the Perfused Brain in Different States of Oxygen Supply", Advances In

Experimental Medicine and Biology Oxygen Transport To Tissue-IV, Vol.159, pp.119-127, 1981

[6] U.Heinrich, J.Hoffmann and D.W.Lubbers, "Quantitative Evaluation of Optical Reflection Spectra of Blood-Free Perfused Guinea Pig Brain Using a Nonlinear Multicomponent Analysis", Pflügers Arch(1987) 409:152-157

[7] J.Hoffmann and D.W.Lubbers, "Quantitative Analysis of Rflection Spectra: Evaluation of Simulated Reflection Spectra".

[8] J.Hoffmann, R.Wodick, F.Hannebauer, and D.W.Lubbers, "Quantitative Analysis of Reflection Spectra of the Surface of the Guinea Pig Brain", Advances In Experimental Medicine and Biology Oxygen Transport To Tissue-V, Vol.169, pp.831-839, 1984

[9] D.W.Lubbers and R.Wodick, "The Examination of Multicomponent Systems in Biological Material by Means of a Rapid Scanning Photometer", Applied Optics, Vol. 8, No.5, pp. 1055-1062, May 1969

[10] D.W.Lubbers, H.H.Figulla, J.Hoffmann and R.Wodick,"The Effect of Hypoxic and histotoxic on Contractility and Blood Flow of the Langendorff Guinea Pig Heart Preparation", Advances In Experimental Medicine and Biology Oxygen Transport To Tissue-IV, Vol.159, pp.225-230, 1981

[11] Dov Malonek and Amiram Grinvald, "Interactions Between Electrical Activity and Cortical Microcirculation revealed by Imaging Spectroscopy: Implications for Functional Brain Mapping", Science, Vol. 272, pp. 551-554, 26 April 1996

[12] J E W Mayhew and Y Zheng, "A Model of the Intrinsic Image Signal and an Evaluation of the Methodology of Intrinsic Image Signal Analysis", Artificial Intelligence Vision Research Unit Report, University of Sheffield, April 1996

[13] A.Seiyama, S.S.Chen, H.Kosaka and T.Shiga, "Microspectroscopic Measurement of the Optical Properties of rat Liver in the Visible Region", Journal of Microscopy, Vol.175, Pt 1, pp. 84-89, July 1994

[14] Setsuo Takatani, Jian Ling, "Optical Oximetry Sensors for Whole Blood and Tissue", IEEE Engineering in Medicine and Biology, pp.347-357, June/July 1994